A W-Band GaN MMIC Continuous 90° Reflective Phase Shifter

Anthony Romano
Department of Electrical Engineering
University of Colorado Boulder
Boulder, CO, USA
anthony.romano@colorado.edu

Timothy Sonnenberg
Department of Electrical Engineering
University of Colorado Boulder
Boulder, CO, USA
timothy.sonnenberg@colorado.edu

Shane Verploegh
ColdQuanta
Boulder, CO, USA
shane.verploegh@colorado.edu

Taylor Barton
Department of Electrical Engineering
University of Colorado Boulder
Boulder, CO, USA
taylor.w.barton@colorado.edu

Zoya Popovic
Department of Electrical Engineering
University of Colorado Boulder
Boulder, CO, USA
zoya@colorado.edu

2022 IEEE 22nd Annual Wireless and Microwave Technology Conference (WAMICON) | 978-1-6654-2195-9/22/$31.00 ©2022 IEEE | DOI: 10.1109/WAMICON53991.2022.9786130

***Abstract*—This paper presents design, simulation, and measurements of a continuous 90° phase shifter implemented in a 40-nm GaN-on-SiC process. The architecture is a reflective phase shifter, which employs a Lange coupler and tunable reactive loads at the "thru" and "coupled" ports. The tunable reactance is implemented with diode-connected HEMTs. Measured results show greater than 90° phase shift across 75–110 GHz with less than 10 dB average loss over a control voltage range of –1 V to +1 V. Simulations use foundry nonlinear device models for the depletion-mode HEMTs, and agree well with measured data across the 75 to 110 GHz range. The extension to a 180° phase shifter is straightforward.**

***Index Terms*—Phase shifter, GaN, W-band.**

I. Introduction

Phased array antennas commonly use phase shifters in feed networks for beam forming and steering [1]. At higher millimeter-wave frequencies, loss and availability of devices presents a challenge for achieving a large phase shift across a wide bandwidth. In this paper, we demonstrate a continuous GaN MMIC phase shifter, shown in Fig. 1, that covers the entire 75–110 GHz W-band.

Phase shifter circuit architectures demonstrated at W-band include digitally switched-delay lines, reactively-loaded lines, and reflective phase shifters [2]. They can be implemented using MEMS [3]–[6], liquid crystals [7], and various integrated semiconductor technologies. Examples in CMOS include [8]–[12], and while these are highly integrated and compact circuits, they suffer from loss due to the substrate, low power handling, and nonlinearity. GaAs phase shifters have also been demonstrated at W-band, e.g. [13], [14]. In transmit phased arrays where higher power levels are required, GaN phase shifters have shown better linearity than GaAs across X-band [15]. The high linearity of GaN is expected at W-band as well, and enables integration with other front-end circuits such as GaN power amplifiers with high power density [16], [17].

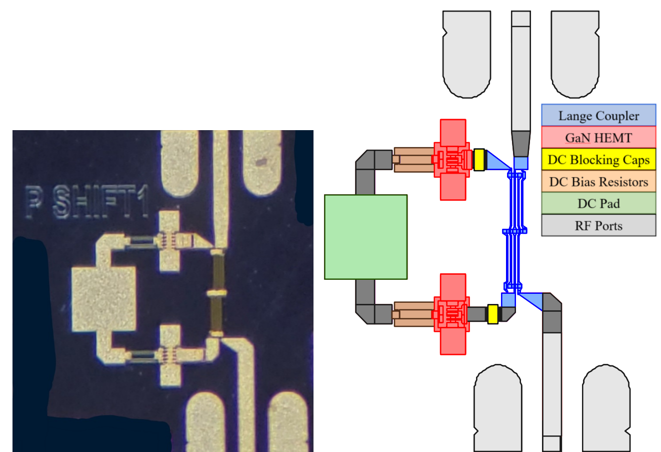

Fig. 1. Photograph (left) and circuit layout (right) of a 0-90° continuous reflective GaN MMIC phase shifter characterized from 75 to 110 GHz. Total size with pads is 1.05 mm by 0.75 mm. The GSG pads have a 100μm pitch.

II. Design of Reflective Phase Shifters in a Millimeter-Wave GaN Process

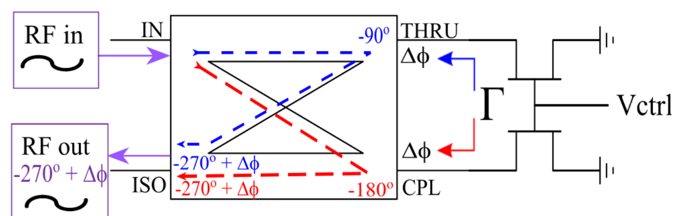

Fig. 2. Schematic of reflective phase shifter with two variable reactances implemented as diode-connected transistors.

Reflective phase shifters allow continuous tuning of phase through reflections from variable loads on two ports of a 90° hybrid coupler. Realizing tunable loads at W-band can be done

Authorized licensed use limited to: UNIVERSITY OF COLORADO. Downloaded on July 19,2022 at 21:35:52 UTC from IEEE Xplore. Restrictions apply.

by connecting HEMTs as varactors. This method is illustrated in Fig. 2. A 3 dB coupler splits the incoming signal power evenly between the "thru" and "coupled" ports. $1/\sqrt{2}$ of the signal arrives at the "thru" port with a $-90°$ phase shift, while the remaining part at the coupled port is shifted by $-180°$. The varactors at the "thru" and "coupled" ports reflect the signal with a tunable phase shift corresponding to the varactor reactance, which is controlled through the gate bias voltage of the HEMT. The two signals then combine constructively at the isolated port with a $-270°$ shift added to the tunable phase. The reflected signals cancel at the input.

The phase shifter design presented here is implemented in the HRL T3 40 nm GaN process on a 50 μm SiC substrate, well documented in [18]. The current T3 process achieves an $f_T/f_{\max}$ of 200/400 GHz with a breakdown voltage greater than 40 V. Three metallization layers are used to form transmission lines and air bridges, while capacitors and resistors are formed with silicon nitride (SiN) and tantalum nitride (TaN), respectively.

An analysis to optimize phase tuning is first performed in order to select the proper HEMT device size. The T3 GaN PDK offers transistors of four standard total peripheries: 50 μm, 150 μm, 300 μm, and 600 μm. Looking into the drain of these sourced-grounded devices, the largest tunable reactance range is found by sweeping the gate voltage from -1 V to $+1$ V. The variable impedance range of these devices is plotted on the Smith Chart in Fig. 3. The 50 μm device is selected for the design, as it provides the greatest tunable reactance magnitude range of 51.4 Ω.

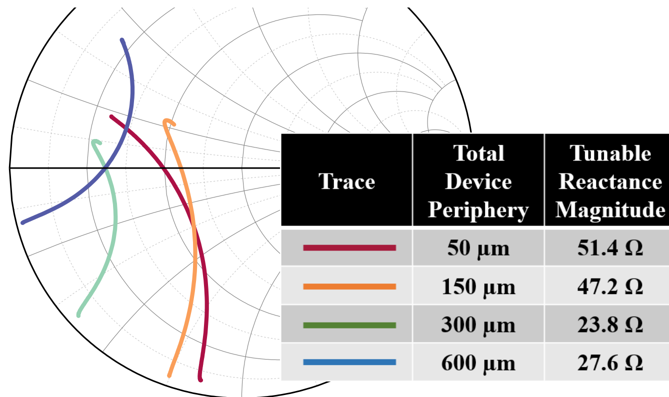

Trace	Total Device Periphery	Tunable Reactance Magnitude
(red)	50 µm	51.4 Ω
(orange)	150 µm	47.2 Ω
(green)	300 µm	23.8 Ω
(blue)	600 µm	27.6 Ω

Fig. 3. Impedance range at 90 GHz looking into the drain of a diode-connected HEMT device for different device peripheries. The traces show variation with control voltage, with the capacitive reactances corresponding to negative gate voltages (devices off).

The second key component of this design is a hybrid coupler. A Lange Coupler is chosen for wideband operation and ease of matching. Furthermore, such a coupler is compact and can be designed in any MMIC process with at least two metal layers. The Lange Coupler used for this design has less than 30 dB of return loss and at least 20 dB of isolation over an octave bandwidth from 60-120 GHz.

The layout of this circuit is displayed in Fig. 1 with the main elements labeled. Two varactors are placed at the "thru" and "coupled" ports of the Lange coupler, with their gates connected to a common bias voltage. Simulated phase states of $0°$, $45°$, and $90°$ are displayed in Fig. 4. The fabricated MMIC phase shifter is captured in the photograph of Fig. 1, and has an overall size of 1.05 mm by 0.75 mm.

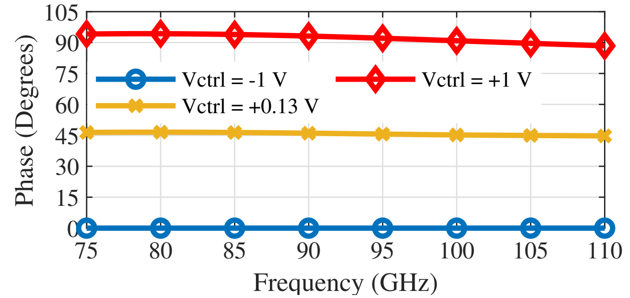

Fig. 4. Three simulated phase states, $0°, 45°$ and $90°$, of the phase shifter versus frequency, corresponding to -1 V, $+0.13$ V and $+1$ V control gate voltages, respectively.

III. Measurements

The fabricated circuits are tested with a calibrated Rohde & Schwarz ZNA vector network analyzer, with ZVA-Z110E millimeter-wave converters for a full W-band characterization (75-110 GHz). Phase, return loss, and insertion loss are captured for each $5°$ increment in phase. The phase states are plotted in Fig. 5, displaying a tunable phase shift ranging from 90° to 105° over the entire bandwidth. $|S_{11}|$ and $|S_{21}|$ for each state are displayed in Fig. 6. Overall, the return loss ranges from 20 to 10 dB, indicating that the device is well matched over the bandwidth. The insertion loss ranges from 2 to 11 dB across all of the phase states.

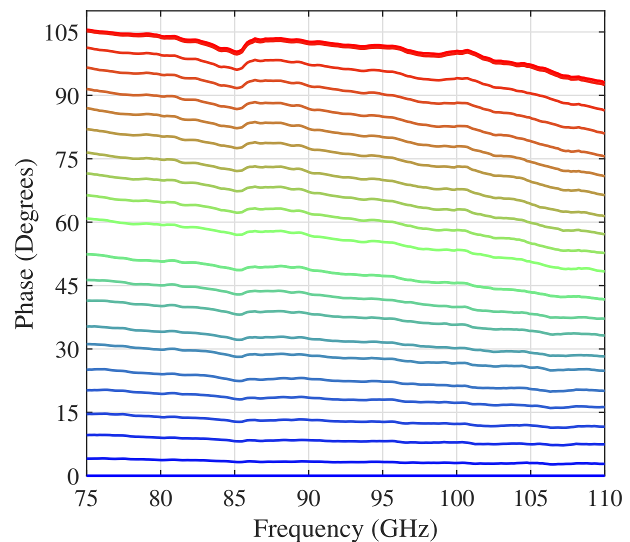

Fig. 5. Measured phase states versus frequency across W band in $5°$ steps, for the gate control voltage from -1 V (blue) to +1 V (red).

Authorized licensed use limited to: UNIVERSITY OF COLORADO. Downloaded on July 19,2022 at 21:35:52 UTC from IEEE Xplore. Restrictions apply.

Phase error is calculated across frequency relative to the phase at 90 GHz. The average measured and simulated phase errors are plotted in Fig. 9. Across the frequency band, the measured phase error is less than 10°, from -6° to +4°, and is within 3° across the band, with the trend well predicted by simulations. The phase shift vs. control voltage is plotted at 75, 90, and 110 GHz to compare the measured and simulated results in Fig. 7. The simulations show a phase shift of up to 90°, while measurements resulted in 105° tunability at the lower end of the band. A comparison for $|S_{21}|$ as a function of control voltage is plotted for three frequencies (upper, lower and center of the band) and is shown in Fig. 8. The insertion loss correlates well between measured and simulated results, although the minimum point is shifted by approximately +0.1 V in the measured data.

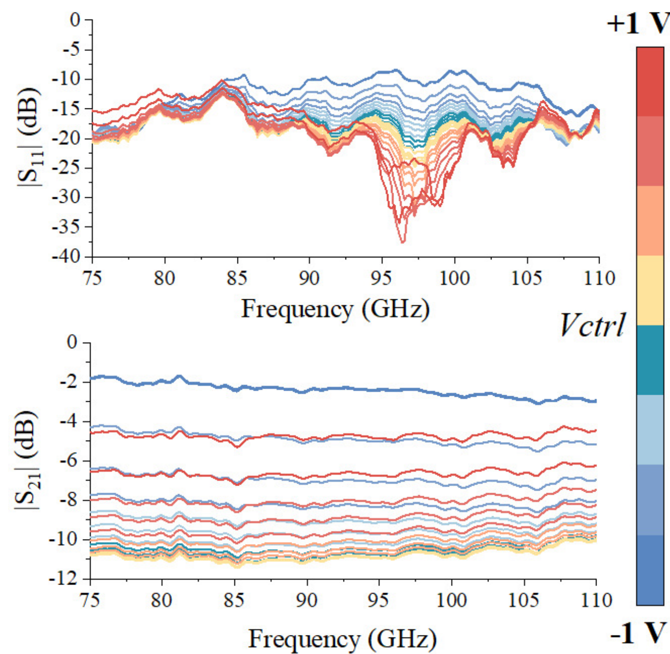

Fig. 6. Measured $|S_{11}|$ (top) and $|S_{21}|$ (bottom) versus frequency as the control voltage is varied from -1 to +1 V.

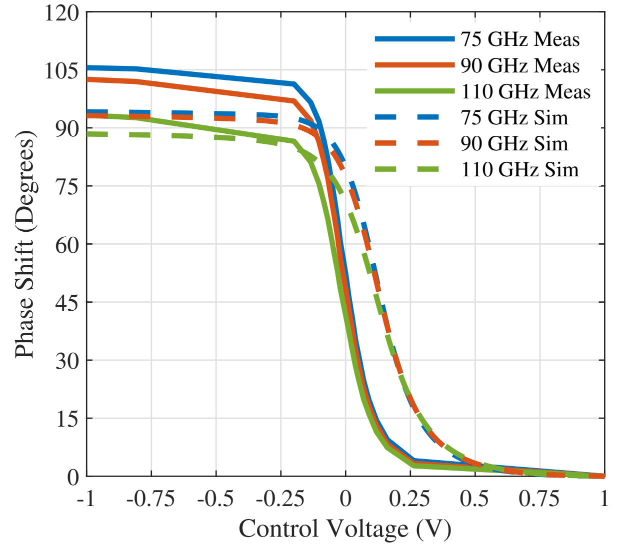

Fig. 7. Measured (solid) and simulated (dashed) phase versus control voltage at 75, 90 and 110 GHz.

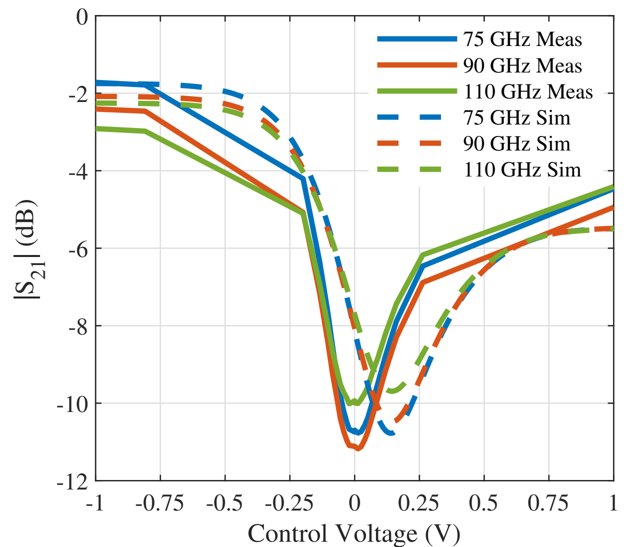

Fig. 8. Measured (solid) and simulated (dashed) $|S_{21}|$ versus control voltage at 75, 90 and 110 GHz.

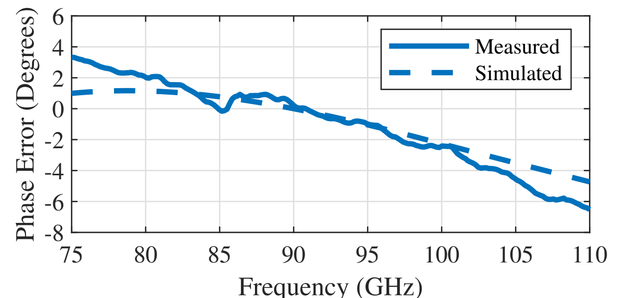

Fig. 9. Measured (solid) and simulated (dashed) phase error vs frequency averaged over all states, relative to the phase at 90 GHz (center of the band).

IV. Conclusion

A greater-than 90° continuous reflective phase shifter is designed and demonstrated across W-band. The GaN MMIC has a measured return loss of less than 10 dB for all phase states, and is not linear with phase (control voltage). The loss is around 2 dB for small and large phase shifts, but increases to around 10 dB when the device impedance is closest to 50 Ω. Given the performance of this device across 75–110 GHz and the good agreement with simulations, we expect that the phase shifter can perform well across an even wider bandwith. However, the available measurement setup does not allow us to capture performance below 75 GHz or beyond 110 GHz currently. For future work, we plan to measure the performance across V band, as well as analyze the power handling and

Authorized licensed use limited to: UNIVERSITY OF COLORADO. Downloaded on July 19,2022 at 21:35:52 UTC from IEEE Xplore. Restrictions apply.

linearity of the device using scalar power measurements. Additionally, we plan to achieve higher degrees of phase shift by cascading several sections of this reflective phase shifter.

REFERENCES

[1] R. R. Romanofsky, "Array phase shifters: Theory and technology," *Antenna Engineering Handbook*, vol. 4, 2007.

[2] S. K. Koul and B. Bhat, *Microwave and millimeter wave phase shifters*. Boston: Artech House, 1991.

[3] N. S. Barker and G. M. Rebeiz, "Optimization of distributed MEMS transmission-line phase shifters-U-band and W-band designs," *IEEE Transactions on Microwave Theory and Techniques*, vol. 48, no. 11, pp. 1957–1966, 2000.

[4] N. Somjit, G. Stemme, and J. Oberhammer, "Binary-coded 4.25-bit W-Band monocrystalline–silicon MEMS multistage dielectric-block phase shifters," *IEEE transactions on microwave theory and techniques*, vol. 57, no. 11, pp. 2834–2840, 2009.

[5] J.-J. Hung, L. Dussopt, and G. M. Rebeiz, "Distributed 2-and 3-bit W-band MEMS phase shifters on glass substrates," *IEEE Transactions on Microwave Theory and Techniques*, vol. 52, no. 2, pp. 600–606, 2004.

[6] D. Psychogiou *et al.*, "Continuously variable W-band phase shifters based on MEMS-actuated conductive fingers," *International Journal of Microwave and Wireless Technologies*, vol. 5, no. 4, pp. 477–489, 2013.

[7] R. Reese *et al.*, "Liquid crystal based dielectric waveguide phase shifters for phased arrays at W-band," *IEEE Access*, vol. 7, pp. 127 032–127 041, 2019.

[8] A. Natarajan *et al.*, "W-Band dual-polarization phased-array transceiver front-end in SiGe BiCMOS," *IEEE Transactions on Microwave Theory and Techniques*, vol. 63, no. 6, pp. 1989–2002, 2015.

[9] H. Li, J. Chen, D. Hou, and W. Hong, "A W-band 6-bit phase shifter with 7 dB gain and 1.35 RMS phase error in 130 nm SiGe BiCMOS," *IEEE Transactions on Circuits and Systems II: Express Briefs*, vol. 67, no. 10, pp. 1839–1843, 2019.

[10] D. Pepe and D. Zito, "Two mm-wave vector modulator active phase shifters with novel IQ generator in 28 nm FDSOI CMOS," *IEEE Journal of Solid-State Circuits*, vol. 52, no. 2, pp. 344–356, 2017.

[11] I. Sarkas *et al.*, "W-band 65-nm CMOS and SiGe BiCMOS transmitter and receiver with lumped IQ phase shifters," in *2009 IEEE Radio Frequency Integrated Circuits Symposium*. IEEE, 2009, pp. 441–444.

[12] H.-S. Lee and B.-W. Min, "W-band CMOS 4-bit phase shifter for high power and phase compression points," *IEEE Transactions on Circuits and Systems II: Express Briefs*, vol. 62, no. 1, pp. 1–5, 2014.

[13] S. Shih *et al.*, "A W-band 4-bit phase shifter in multilayer scalable array systems," in *2007 IEEE Compound Semiconductor Integrated Circuits Symposium*. IEEE, 2007, pp. 1–4.

[14] J. G. Yang, J. Lee, and K. Yang, "A W-band InGaAs PIN-MMIC digital phase-shifter using a switched transmission-line structure," in *2012 International Conference on Indium Phosphide and Related Materials*. IEEE, 2012, pp. 99–101.

[15] M. Robinson, P. Danielson, and Z. Popović, "Continuous broadband GaAs and GaN MMIC phase shifters," *IEEE Microwave and Wireless Components Letters*, 2021.

[16] A. Margomenos *et al.*, "GaN technology for E, W and G-band applications," in *2014 IEEE compound semiconductor integrated circuit symposium (CSICS)*. IEEE, 2014, pp. 1–4.

[17] ——, "W-Band GaN receiver components utilizing highly scaled, next generation GaN device technology," in *2014 IEEE Compound Semiconductor Integrated Circuit Symposium (CSICS)*, 2014, pp. 1–4.

[18] K. Shinohara *et al.*, "Scaling of GaN HEMTs and schottky diodes for submillimeter-wave MMIC applications," *IEEE Transactions on Electron Devices*, vol. 60, no. 10, pp. 2982–2996, 2013.

Authorized licensed use limited to: UNIVERSITY OF COLORADO. Downloaded on July 19,2022 at 21:35:52 UTC from IEEE Xplore. Restrictions apply.